CONF-790507--4

MASTER

POSSIBLE VISCOSITY EFFECTS IN NEUTRON-INDUCED FISSION OF ^{232}Th AND ^{238}U

by

J.E. Gindler, L.E. Glendenin and B.D. Wilkins

Prepared for

4th IAEA Symposium

on

Physics and Chemistry of Fission

Julich, Germany

May 14-18, 1979

U of C-AUA-USDOE

ARGONNE NATIONAL LABORATORY, ARGONNE, ILLINOIS

Operated under Contract W-31-109-Eng-38 for the
U. S. DEPARTMENT OF ENERGY

DISCLAIMER

IAEA-SM/241-F5. POSSIBLE VISCOSITY EFFECTS IN NEUTRON-INDUCED FISSION OF ^{232}Th and ^{238}U†

J. E. Gindler, L. E. Glendenin and B. D. Wilkins
Chemistry Division, Argonne National Laboratory
9700 South Cass Avenue, Argonne, Illinois 60439
U.S.A.

ABSTRACT

Fission yields induced in the ^{238}U(n,f) and ^{232}Th(n,f) reactions have been determined as a function of incident neutron energy (E_n). The ratio of ^{115}Cd-to-^{140}Ba yields as a function of E_n is analyzed in the present paper by means of the equation $Y_1/Y_2 = \exp[2(a_1(E_n+E_1)^{\frac{1}{2}} - 2(a_2(E_n+E_2)^{\frac{1}{2}}]$ to give values of a_i, the level density parameter, and E_i, the excitation energy for E_n=0. The energies E_i are interpreted on the basis of the liquid drop model with shell and pairing corrections. Values are deduced for the energy dissipated by viscosity effects in the descent from the saddle point to the point where masses are fixed in the fissioning nucleus. These values are 1.7 MeV for ^{232}Th(n,f) and 4.8 MeV for ^{238}U(n,f). These values are consistent with the experimental observation that $\bar{\nu}_p$ is ∿0.6 neutron greater for ^{239}U fission than for ^{233}Th fission and that strong odd-even (nucleon pairing) effects are found in the fragment total kinetic energy distribution for ^{230}Th fission but not for ^{234}U fission. The low dissipation energy values together with the low values of pre-scission kinetic energy deduced by Guet, et al. [Nucl. Phys. A134 (1971)1] indicate a shorter path from the saddle point of the fissioning nucleus to scission than is generally assumed in theoretical calculations.

1. INTRODUCTION

One of the most perplexing problems in fission today is the degree of adiabaticity in the descent of the nucleus from the saddle point to scission. That is, how much of the potential energy release from saddle to scission appears as nuclear dissipation energy and how much appears as pre-scission kinetic energy? Dynamic calculations [1-3] give a wide range of values for the two energies depending on the initial assumptions made concerning the dissipation mechanism, i.e., two-body viscosity, one-body viscosity, etc. The problem remains since the scission configuration

†Work performed under the auspices of the Office of Basic Energy Sciences of the Department of Energy.

cannot be uniquely determined from experimental measurements of total kinetic energy and excitation energy which are measured at essentially infinite distances between the fragments.

Another experiment that in principle should provide information on the amount of energy dissipated is the measurement of near-symmetric fission yields as a function of incident neutron energy (E_n). Analyses of such yields have been made previously but with different objectives: to measure the effect of angular momentum [4], the effect of excitation energy [5], or the effect of the level density parameter [5,6]. The measurement of such yields is part of a broader program to determine the post-neutron-emission mass distributions for fissile and fertile nuclides as a function of E_n underway at Argonne National Laboratory for the past several years. Experimental results are presently available for $^{238}U(n,f)$ [7,8] and $^{232}Th(n,f)$ [9] with neutron energies from 1.5 to 8 MeV.

In view of the success of the quasistatistical scission-point model of fission [10] in interpreting mass and total kinetic energy (TKE) distributions for a wide variety of fissioning systems, it is proposed that the variation of the near-symmetric fission yeilds for ^{239}U and ^{233}Th compound nuclei be explained in terms of such a model. It is assumed that fission masses are fixed at some point between the saddle and scission points and that a quasistatistical equilibrium is attained at this point. Assuming the level density to be described by a Fermi gas, the density of excited states to which the fission yield is related is given by [11]

$$N = k(E^*) \exp(2\sqrt{aE^*}) , \qquad (1)$$

where E^* is the excitation energy at the point where masses are fixed and a is the level density parameter. The ratio of two fission yields is then

$$Y_1/Y_2 = (k_1(E_1^*)/k_2(E_2^*)) \exp(2\sqrt{a_1E_1^*} - 2\sqrt{a_2E_2^*}). \qquad (2)$$

The use of Eq. (2), which is also that used by Fong [11] in his statistical approach to nuclear fission, does not necessarily imply a situation of complete damping in the descent of the nucleus from the saddle to the point at which masses are final. Rather, it is assumed that a weak coupling exists between collective and intrinsic states as described by Nörenberg [12].

The excitation energy E_i^* is defined as

$$E_i^* = E_n + B_n - B_f - E_{LDi} + E_{DIS} + \Delta E_{SPi} \exp[-(T_i/T_o)^2]. \qquad (3)$$

The first three terms are respectively the kinetic energy of the neutron, its binding energy in the compound nucleus, and the fission barrier height of the compound nucleus. All of these terms are known for ^{239}U and ^{233}Th [13]. The liquid drop term E_{LDi} is the energy required to form a pair of fragments other than the symmetric pair since the latter is the favored configuration in the liquid drop model. The value of this term is obtained from liquid drop calculations. The quantity E_{DIS} represents the unknown amount of dissipation energy at the point where masses are determined. The ΔE_{SPi} term includes the microscopic single-particle corrections for shell and pairing effects. The magnitude of the shell correction determined in the scission-point model of fission is shown for neutrons in Fig. 1 and for protons in Fig. 2 [10]. Although these corrections are for independent fragments, they are comparable to the single-particle shell corrections obtained with the two-center model [14]. The shell corrections shown in Figs. 1 and 2 are for $E_i^*=0$. The variation of the shell correction with intrinsic temperature of the nucleus is shown in Fig. 3 for neutrons at a fixed (0.65) β-deformation [10]. These functions were calculated with the approximation described by Jensen and Damgaard [15]. The more simplified temperature correction, $\exp[-(T_i/T_o)^2]$, given in Eq. (3) is one suggested by Ziegenhain, et al., [16]. In this expression $T = (E_i^*/a_i)^{1/2}$ and $T_o = 1.5$ MeV. Although the pairing correction exhibits a different temperature dependence [17] than do the shell corrections, the latter are generally larger in magnitude. Therefore, since one will not be able to distinguish between pairing and shell corrections, a temperature-dependence correction suitable for the latter is applied.

Because of the temperature (or E_i^*) dependence of ΔE_{SPi} and its unknown relationship with E_n, the excitation energy E_i^* as defined in Eq. (3) is some convoluted function of itself. Therefore, a series of equations of the form of Eq. (2) cannot be solved explicitly for E_i^*. If, however, ΔE_{SPi} varies slowly over the E_n range of the analysis, then a least-squares fit to the data should yield reasonable values of E_i^* and, consequently, E_{DIS}. In the present paper we have assumed this slow variation and that the values of ΔE_{SPi} obtained are most relevant to the mid-point of the E_n range or ∿4.5 MeV.

2. EXPERIMENT

The experimental method is described more completely in Ref. [7]. Metallic foils of thorium or uranium were irradiated with essentially monoenergetic neutrons produced by the $^7Li(p,n)^7Be$ or $^2H(d,n)^3He$ reactions. The induced fission product activities were analyzed by means of γ-ray spectrometry or radiochemical techniques. After applying appropriate corrections for chemical yield or γ-ray abundance, detection efficiency, decay, genetic relationships, and degree of saturation, absolute yields were calculated by normalizing the resulting mass distributions to 200% total yield.

The results of these measurements for near-symmetric fission masses are shown in Fig. 4 for ^{239}U and in Fig. 5 for ^{233}Th. The results of Ford and Leachman [4], Borisova, et al., [5] and Adams, et al., [18] are also shown in Fig. 4. The results of Turkevich, Niday and Tompkins [19], Ford and Leachman [4] and Dubrovina, et al., [6] are also shown in Fig. 5. An average value of the 14-MeV neutron yields given by Crouch [20] and Meek and Rider [21] is plotted in Fig. 5.

The yields (Y) of the near-symmetric fission masses increase rapidly with E_n for both ^{239}U and ^{233}Th with those for ^{233}Th increasing more rapidly initially. The onset of second-chance fission in ^{239}U is marked by a pronounced change in slope of the Y vs. E_n curves and perhaps by a slight dip. In ^{233}Th a definite dip occurs at those energies where second-chance fission becomes possible. The onset of third-chance fission in both fissioning systems is marked by another change in slope of the Y vs. E_n curves. In Fig. 6 the Y vs. E_n curves of the valley fission product ^{115}Cd are compared for both ^{233}Th and ^{239}U.

In contrast to the near-symmetric fission mass yields, those of asymmetric masses near the peaks in the mass distribution decrease slightly with increasing E_n for ^{239}U. This is shown for ^{99}Mo in Fig. 4. The yield behavior with E_n of the corresponding masses for ^{233}Th is more complex as seen in Fig. 7. This shows that the yields of masses more asymmetric than the peak-yield masses increase sharply at the onset of second-chance fission; whereas the yields of more symmetric masses decrease sharply.

3. ANALYSIS

In analyzing the data, first-chance fission yields were calculated for neutron energies at which both first- and second-chance fission could occur. This was done by use of the measured fission cross sections (σ_F) for ^{233}Th [22] and ^{239}U [23] as shown in Fig. 6. The measured yields at these energies may be written as

$$Y(E_n) = \frac{\sigma_{F-I}}{\sigma_F} Y_I(E_n) + \frac{\sigma_{F-II}}{\sigma_F} Y_{II}(E_n - \varepsilon_n), \qquad (4)$$

where the subscripts I and II refer respectively to first- and second-chance fission. The second-chance fission yield Y_{II} is evaluated in the first-chance fission energy region ($E_n - \varepsilon_n$), where ε_n ($\sim$6 MeV) is the sum of the binding energy and kinetic energy of a neutron emitted from the compound ^{233}Th or ^{239}U nucleus prior to fission. This analysis assumes that the fission yield from an excited ^{232}Th or ^{238}U nucleus is the same as that from an excited ^{233}Th or ^{239}U nucleus at the same incident neutron energy, ($E_n - \varepsilon_n$). Values of σ_{F-I} were obtained by extrapolating horizontally the fission cross section σ_F vs. E_n curve just prior to the onset of second-chance fission. This gives values of 0.14 barn for ^{233}Th and 0.56 barn for ^{239}U. Such a procedure is fairly straightforward for ^{239}U since the fission cross section curve is a fairly flat plateau in the energy region where only first-chance fission occurs. However, the fission cross section curve for ^{233}Th exhibits some structure in the energy region for which only first-chance fission occurs. There is, therefore, some ambiguity associated with the value of 0.14 barn used for σ_{F-I}. Values of σ_{F-II} were deduced by subtracting σ_{F-I} from σ_F. Values of Y_I were then calculated by substituting the above quantities into Eq. (4). The dashed curve in Fig. 6 indicates the calculated first-chance ^{115}Cd yield for ^{233}Th.

The ratio of ^{115}Cd-to-^{140}Ba yields for first-chance fission of the thorium and uranium systems are shown as circles in Fig. 8. Open circles are the result of measured first-chance fission yields. Solid circles are the result of first-chance fission yields deduced by means of Eq. (4). For comparison the results of Dubrovina, et al., [6] for ^{115}Cd-to-^{89}Sr yields are given as open triangles for ^{233}Th. The results of Borisova, et al., [5] for ^{115}Cd-to-½(^{99}Mo + ^{140}Ba) yields are given as solid triangles for ^{239}U. Since the ratio of ^{140}Ba-to-^{89}Sr yields averages 1.15 in the region where only first-chance fission occurs for ^{232}Th [6] and the ratio of ^{99}Mo-to-^{140}Ba yields averages 1.13 in the corresponding region for ^{238}U [5], the present data are seen to agree very well with the data of Refs. 5 and 6.

Although Eq. (2) applies to yields of pre-neutron-emission fission fragments, it is assumed that the yields of the post-neutron-emission fission products ^{115}Cd and ^{140}Ba represent well the yields of pre-neutron-emission progenitors which are assumed for simplicity to be respectively ^{117}Rh and ^{141}Xe. The respective complements of these fragments are ^{116}Rh and ^{92}Kr for ^{232}Th(n,f) and ^{122}Ag and ^{98}Sr for ^{238}U(n,f).

In applying Eq. (2) to the data shown in Fig. 8 it was assumed that the pre-exponential factor $k_1(E_1^*)/k_2(E_2^*)$ was equal to one. The level density parameter was defined as $a_i = A_f/c_i$, where A_f is the mass of the fissioning nucleus, and c_i is a constant $\approx$10. The values of c_i were constrained to be the same for both ^{233}Th and ^{239}U. This is reasonable since, for ^{141}Xe (the ^{140}Ba progenitor), the shell effects are the same for both fissioning systems (point H in Fig. 1) and the complementary fragments are found at a β-deformation of 0.4 (near point B in Fig. 1) [10]. Similarly, for ^{117}Rh (the ^{115}Cd progenitor), the shell effects are the same for both fissioning systems at a β-deformation of 0.7, and the complementary fragments are found at the same deformation (to the right of point D in Fig. 1). The larger deformations for the near-symmetric fission fragments is indicated by the dip in the total kinetic energy near symmetry observed in the fission of both ^{232}Th [24] and ^{238}U [25,26] by energetic neutrons, assuming a small pre-scission kinetic energy. Rewriting E_i^* as $E_n + E_i$, Eq. (2) then becomes

$$Y_1/Y_2 = \exp\left[2\left((A_f/c_1)\cdot(E_n+E_1)\right)^{\frac{1}{2}} - 2\left((A_f/c_2)\cdot(E_n+E_2)\right)^{\frac{1}{2}}\right]. \qquad (5)$$

Application of Eq. (5) simultaneously to the uranium and thorium data gave the preliminary least-squares best fits shown by the solid curves in Fig. 8. Values of the parameters c_i, a_i, and E_i obtained for ^{233}Th and ^{239}U are given in Table I. The values of a_1, a_2, E_1, and E_2 determined for ^{239}U are significantly smaller than the respective values of 31.1, 27.4, 3.6, and 7.1 obtained by Borisova, et al., [5]. Their energies, E_1 and E_2, are reported as "corresponding to the fission threshold of ^{238}U, that is, for E_n=1.5 MeV." Substituting their values into Eq. (5) does not give a good fit to the data. The least squares fit to the level density parameter, a_i, gives quite reasonable values of $A_f/9.59$ and $A_f/11.35$ for the symmetric and asymmetric mass splits, respectively.

Since $E_i = E_i^* - E_n$, Eq. (3) can be rearranged to give

$$E_i - B_n + B_f + E_{LDi} = E_{DIS} - \Delta E_{SPi}(T). \qquad (6)$$

The measured or calculated quantities on the left-hand side of Eq. (6) are listed in Table II. The values of $E_{DIS}-\Delta E_{SPi}(T)$ at $E_n \sim$4.5 to 5 MeV are also given in Table II. The values of $\Delta E_{SP_1}(T)-\Delta E_{SP_2}(T)$ listed in the table are obtained by subtracting the two values of $E_{DIS}-\Delta E_{SPi}(T)$ for a given fissioning system. To determine E_{DIS} an estimate of $\Delta E_{SPi}(T)$ is needed. Values were taken from data described by the scission-point model of fission [10] and are listed below the dashed line in Table II. However, these calculated values are appropriate for E_i^*=0. (The experimental values are for $E_i^* \simeq 4.5 + E_i$ MeV.) Therefore, the calculated values were corrected to correspond to the experimental excitation energies. The temperature-corrected values, $\Delta E_{SPi}(T)$ and $\Delta E_{SP_1}(T)-\Delta E_{SP_2}(T)$ are given in Table III. The calculated and experimentally derived values of $\Delta E_{SP_1}(T)-\Delta E_{SP_2}(T)$ agree to within 7% for ^{233}Th and 12% for ^{239}U. This agreement is rather gratifying in view of the uncertainties in the Strutinski method for calculating shell effects for deformed nuclear shapes [27] and the use of an independent fragment model [10] for their derivation. To bring the calculated values of $\Delta E_{SPi}(T)$ into agreement with the experimental values, the former were normalized to give the experimentally derived values of $\Delta E_{SP_1}(T)-\Delta E_{SP_2}(T)$. These values are listed in Table III. Adding the normalized values of $\Delta E_{SPi}(T)$ to the values of $E_{DIS}-\Delta E_{SPi}(T)$ given in Table II yields E_{DIS} values of 1.7 MeV for ^{233}Th and 4.8 MeV for ^{239}U, a difference of 3.1 MeV.

4. DISCUSSION

A number of assumptions have been made in the above analyses that affect the accuracy of the deduced E_{DIS} values for the ^{233}Th and ^{239}U compound nuclei. Certainly one may question the applicability of the Fermi gas level density at such low values of E_i^*. Nevertheless, the data cannot be fit with large values of E_{DIS}. Therefore, the picture of complete damping between the saddle point and the point where masses are fixed appears to be eliminated. The values obtained for E_{DIS} are also consistent with the discussion on pairing in the scission-point model [10] which attributes the strong odd-even effect observed in the TKE distribution for the fission of ^{229}Th with thermal neutrons, shown in Fig. 9 [28], to the very low scission-point temperature expected in thorium systems.

The difference of 3.1 MeV between values of E_{DIS} for ^{239}U and ^{233}Th is much less sensitive to the assumptions made and can, in fact, be seen directly in the data before analysis (see Fig. 6). The 3.1 MeV E_{DIS} difference between ^{239}U and ^{233}Th is also consistent with the difference between $\bar{\nu}_p$ for the two nuclides, which is ∿0.6 neutron for a given incident neutron energy [29]. Since the number of neutrons emitted per fission is a measure of E_{DIS} plus the average fragment deformation energy and the difference in $\bar{\nu}_p$ between ^{239}U and ^{233}Th is accounted for by the difference in E_{DIS}, one may conclude that the deformation energies at the scission point for these two fissioning systems are approximately equal. Guet, et al., [30] in a study of long-range alpha particles in ^{235}U(n,f), decide that only a compact scission shape with relatively low pre-scission kinetic energy (<10 MeV) is consistent with their data. If pre-scission kinetic energy is small, then the total kinetic energy is dominated by the post-scission kinetic energy. The latter can be approximated by

$$(\mathrm{TKE})_{\mathrm{post}} = Z_1 Z_2 e^2/D, \qquad (7)$$

where D is the distance between the charge centers at scission. Since the total deformation energy is shown to be equal for ^{233}Th and ^{239}U, then D should also be nearly equal for systems which are so similar. One may therefore calculate the expected TKE differences for the most probable charge divisions (Z = 54 and 38 for ^{239}U and Z = 54 and 36 for ^{233}Th). This amounts to a 5.6% difference or ∿9 MeV for compact scission shapes deduced by Guet, et al., [30]. Experimental values of $\overline{\mathrm{TKE}}$ are ∿172.5 MeV for ^{239}U [26] and ∿163 MeV for ^{233}Th [24], a 5.8% difference or 9.5 MeV. The 0.5-MeV difference between the calculated and experimental energies indicates very little difference in the pre-scission kinetic energy for the two fissioning systems. Since all dynamic calculations that predict appreciable amounts of pre-scission kinetic energy indicate a strong dependence on the parameter $Z^2/A^{1/3}$ in the actinide region of the elements [31], one concludes that the pre-scission kinetic energy is small, i.e., less than 10 MeV, consistent with Guet, et al. [30].

In view of the experimental evidence we conclude that fission occurs with small amounts of dissipation energy, small amounts of pre-scission kinetic energy, and compact shapes at the scission point. Such a situation is incompatible with current dynamic calculations. Original one-body viscosity calculations yield compact shapes but large amounts of E_{DIS} and essentially no pre-scission kinetic energy [3]. Two-body viscosity calculations give very extended shapes with varying but always large amounts of pre-scission kinetic energy [2,3]. In Fig. 10 is shown the potential energy surface for ^{236}U as a function of neck constriction and total elongation of the system. This figure was taken from the recent paper by Negele, et al., [3] on fission dynamics. Two valleys in the potential energy surface are apparent in the figure. The upper valley is quite flat descending from the second saddle point and exhibits stability against constriction of the neck. This valley leads to the extended shapes at scission predicted by the two-body viscosity calculations. The lower valley is associated with approaching fragments in heavy ion reactions. It exhibits little stability against neck constriction and can lead to more compact shapes at scission. A small ridge separates the two valleys. At elongations greater than 17 fm ($\sim 2.25/AR_0^2$ units), the potential energy of the lower valley becomes less than that of the upper valley. Also, the upper valley is very flat in the region of 17-18 fm, exhibiting a slight saddle point. This is similar to the scission saddle described by Nörenberg [12] where the attractive forces of the neck balance or even over-balance the repulsive Coulomb force. Davies, et al., [31] show that rupture occurs for neck thicknesses of $\sim$2 fm. Previous calculations assumed that scission occurs for zero neck thicknesses. The experimental evidence of small dissipation energy, small pre-scission kinetic energy, and compact shapes together with the 2-fm neck thickness indicate that scission occurs at $\eta \approx .68$ and $Q \approx 2.4$, indicated by an x in Fig. 10. This corresponds to a separation between charge centers of 17-18 fm. The approximate energy release from the second saddle to this scission position for ^{236}U is $\sim$9 MeV, in good agreement with the presently proposed sum of dissipation energy and pre-scission kinetic energy for ^{239}U. It is suggested that dynamical calculations be undertaken to determine whether the fissioning system can be diverted from the upper valley in the region of the third saddle point, i.e., 17-18 fm, to the lower valley where scission can occur with parameters more consistent with those derived from experiment.

REFERENCES

[1] KOONIN, S.E., NIX, J.R., Phys. Rev. C 13 (1976) 209.

[2] DAVIES, K.T.R., SIERK, A.J., NIX, J.R., Phys. Rev. C 13 (1976) 2385.

[3] NEGELE, J.W., KOONIN, S.E., MÖLLER, P., NIX, J.R., SIERK, A.J., Phys. Rev. C 17 (1978) 1098.

[4] FORD, G.P., LEACHMAN, R.B., Phys. Rev. 137 (1965) 826.

[5] BORISOVA, I., DUBROVINA, S.M., NOVGRODTSEVA, V.I., PECHLIN, V.A., SHIGIN, V.A., SHUBKO, V.M., Yad, Fiz. 6 (1967) 454 [Sov. J. Nucl. Phys. 6 (1968) 331].

[6] DUBROVINA, S.M., NOVGRODTSEVA, V.I., MOROZOV, L.N., PECHLIN, V.A., CHISTYAKOV, L.V., SHIGIN, V.A., SHUBKO, V.M., Yad. Fiz. 17 (1973) 470 [Sov. J. Nucl. Phys. 17 (1973) 240].

[7] NAGY, S., FLYNN, K.F., GINDLER, J.E., MEADOWS, J.W., GLENDENIN, L.E., Phys. Rev. C 17 (1978) 163.

[8] GINDLER, J.E., GLENDENIN, L.E., MEADOWS, J.W., Nucl. Sci. Eng. 70 (1979) 101.

[9] GLENDENIN, L.E., GINDLER, J.E., AHMAD, I., MEADOWS, J.W., Abstracts of Papers, American Chemical Society, 177th National Meeting, Honolulu, Hawaii, April 2-6, 1979, NUCL-4.

[10] WILKINS, B.D., STEINBERG, E.P., CHASMAN, R.R., Phys. Rev. C 14 (1976) 1832.

[11] FONG, P., Statistical Theory of Nuclear Fission, Gordon and Breach, New York (1969).

[12] NÖRENBERG, W., Physics and Chemistry of Fission (Proc. 2nd IAEA Symp., Vienna, 1969) IAEA, Vienna (1969) 51.

[13] MYERS, W.D., SWIATECKI, W.J., Nuclear Masses and Deformations, Lawrence Radiation Laboratory Rep. UCRL-11980 (1965).

[14] MOSEL, U., SCHMITT, H.W., Phys. Rev. C 4 (1971) 2185.

[15] JENSEN, A.S., DAMGAARD, J., Nucl. Phys. A203 (1973) 578.

[16] ZIEGENHAIN, K.H., LUSTIG, H.J., HAHN, J., MARUHN, J.A., GREINER, W., SCHEID, W., Fizika 9 suppl. 4 (1977) 559.

[17] MORETTO, L.G., Phys. Lett. 40B (1972) 1.

[18] ADAMS, D.E., JAMES, W.D., BECK, J.N., KURODA, P.K., J. Inorg. Nucl. Chem. 37 (1975) 419.

[19] TURKEVICH, A., NIDAY, J.B., TOMPKINS, A., Phys. Rev. 89 (1953) 552.

[20] CROUCH, E.A.C., At. Data Nucl. Data Tables 19 (1977) 419.

[21] MEEK, M.E., RIDER, B.F., Compilation of Fission Product Yields, NEDO-12154-2, Vallecitos Nuclear Center (1977).

[22] MEADOWS, J., POENITZ, W., SMITH, A., SMITH, D., WHALEN, J., HOWERTON, R., Evaluated Nuclear Data File of Th-232, Argonne National Laboratory Rep. ANL-NDM-35 (1978).

[23] POENITZ, W., PENNINGTON, E., SMITH, A.B., HOWERTON, R., Evaluated Fast Neutron Cross Sections of Uranium-238, Argonne National Laboratory Rep. ANL-NDM-32 (1977).

[24] SERGACHEV, A.I., VOROB'EVA, V.G., KUZ'MINOV, B.D., MIKHAILOV, V.B., TARASKO, M.Z., Yad. Fiz. 7 (1968) 778 [Sov. J. Nucl. Phys. 7 (1968) 475].

[25] SINCHENKO, V.I., SERGACHEV, A.S., MIKHAILOV, V.B., VOROB'EVA, V.G., TARASKO, M.Z., KUZ'MINOV, B.D., Yad. Fiz. 6 (1968) 708 [Sov. J. Nucl. Phys. 6 (1968) 516].

[26] VOROB'EVA, V.G., KUZ'MINOV, B.D., SERGACHEV, A.I., TARASKO, M.Z., Yad. Fiz. 9 (1969) 296 [Sov. J. Nucl. Phys. 9 (1969) 175].

[27] STRUTINSKI, V.M., Nucl. Phys. A95 (1967) 420.

[28] UNIK, J.P., GINDLER, J.E., GLENDENIN, L.E., FLYNN, K.F., GORSKI, A., SJOBLOM, R.K., Physics and Chemistry of Fission (Proc. 3rd IAEA Symp., Rochester, N.Y., 1973) 2, IAEA, Vienna (1974) 19.

[29] MANERO, F., KONSHIN, V.A., At. Energy Rev. 10 (1972) 637.

[30] GUET, C., SIGNARBIEUX, C., PERRIN, P., NIFENECKER, H., ASHGAR, M., CAITUCOLLI, F., LEROUX, B., Nucl. Phys. A314 (1979) 1.

[31] DAVIES, K.T.R., MANAGAN, R.A., NIX, J.R., SIERK, A.J., Phys. Rev. C 16 (1977) 1890.

FIGURE CAPTIONS

FIG. 1. Neutron-shell corrections calculated as a function of β-deformation and neutron number. The β-parameter is defined in terms of the semimajor (c) and semiminor (a) axes of a prolate spheroid with $c = kr_0A^{1/3}(1+2\beta/3)$ and $a = kr_0A^{1/3}(1-\beta/3)$, where k is a volume conservation factor. The contours are plotted as 1 MeV intervals with the black regions (representing the strongest shells) containing all values less than -4 MeV and the inner white region (representing the weakest shell corrections) containing all values greater than +2 MeV. From Ref. [10].

FIG. 2. Proton-shell corrections calculated as a function of β-deformation and proton number. Contour strengths are described in the caption for Fig. 1. From Ref. [10].

FIG. 3. Neutron-shell corrections at fixed deformation (β = 0.65) calculated as a function of the temperature of the nucleus. From Ref. [10].

FIG. 4. Fission yields and cross section σ_F for fission of ^{238}U by monoenergetic neutrons as a function of neutron energy. From Ref. [7].

FIG. 5. Fission yields of near-symmetric masses for fission of ^{232}Th by monoenergetic neutrons as a function of neutron energy.

FIG. 6. Fission yield of the valley fission product ^{115}Cd and the fission cross section σ_F as a function of neutron energy for ^{232}Th(n,f) and ^{238}U(n,f). The dashed curve (---) represents the first-chance fission yield of ^{115}Cd for ^{232}Th(n,f) calculated for $E_n > 6$ MeV.

FIG. 7. Fission yields of asymmetric masses for fission of ^{232}Th by monoenergetic neutrons as a function of neutron energy. The yields of complementary masses are shown assuming three neutrons are emitted per fission event.

FIG. 8. Ratio of symmetric-to-asymmetric yields for first-chance fission of ^{233}Th and ^{239}U as a function of neutron energy. Circles are present data and represent the ratio of ^{115}Cd-to-^{140}Ba yields. Open circles are for yields measured in the energy region for which only first-chance fission occurs. Solid circles are for yields deduced by the method described in the text. Open triangles are the data of Ref. [6] and represent the ratio of ^{115}Cd-to-^{89}Sr yields. Solid triangles are the data of Ref. [5] and represent the ratio of ^{115}Cd-to-½(^{99}Mo + ^{140}Ba) yields. The solid curves are fits to the present data by means of Eq. (5).

FIG. 9. Average total kinetic energy for thermal neutron induced fission of ^{229}Th as a function of primary heavy-fragment mass. The dashed curve in (b) shows TKE(A) values for the thermal neutron induced fission of ^{233}U multiplied by 0.944. The curve shown in (a) represents the differences between the two curves shown in (b). From Ref. [28].

FIGURE CAPTIONS (Cont'd)

FIG. 10. Contours in the Q-η plane of the microscopic-macroscopic potential energy of ^{236}U with zero spin-orbit interaction, in units of MeV. The scission point suggested in the present paper is denoted by an X. From Ref. [3].

TABLE I. Parameters obtained for Eq. (5) in its fit to first-chance fission data.

Parameter	$^{232}Th(n,f)$	$^{238}U(n,f)$
c_1	9.59 amu/MeV	9.59 amu/MeV
c_2	11.35 amu/MeV	11.35 amu/MeV
$a_1=A_f/c_1$	24.3 MeV^{-1}	24.9 MeV^{-1}
$a_2=A_f/c_2$	20.5 MeV^{-1}	21.0 MeV^{-1}
E_1	-0.5 MeV	2.4 MeV
E_2	2.6 MeV	6.8 MeV

TABLE II. Energies used in Eq. (6).

Energy	^{232}Th(n,f) (MeV)	^{238}U(n,f) (MeV)
B_n	4.955[a]	4.783[a]
B_f	6.44[b]	6.15[b]
E_{LD1}	0.01[c]	0.06[e]
E_{LD2}	2.72[d]	1.91[f]
E_1[g]	-0.5	2.4
E_2[g]	2.6	6.8
$E_{DIS}-\Delta E_{SP1}(T)$[h]	0.995	3.83
$E_{DIS}-\Delta E_{SP2}(T)$[h]	6.805	10.08
$\Delta E_{SP1}(T)-\Delta E_{SP2}(T)$[i]	5.81	6.25
$\Delta E_{SP1}(T)$[j]	.69	1.19
$\Delta E_{SP2}(T)$[j]	-5.62	-7.78
$\Delta E_{SP1}(T)-\Delta E_{SP2}(T)$[k]	6.31	8.97

[a]Values determined from experimental masses given in Ref. [13].

[b]Experimental values given in Table II of Ref. [13].

[c]Calculated for a 117/116 mass split in ^{233}Th.

[d]Calculated for a 141/92 mass split in ^{233}Th.

[e]Calculated for a 122/117 mass split in ^{239}U.

[f]Calculated for a 141/98 mass split in ^{239}U.

[g]Values from the present work assumed valid for $E_n \gtrsim$ 4.5 MeV.

[h]Calculated by means of Eq. (6).

[i]Calculated by subtracting values of $E_{DIS}-\Delta E_{SPi}(T)$ for a given fissioning system.

[j]Values based on the scission-point model of fission described in Ref. [10].

[k]Calculated by subtracting values of $\Delta E_{SPi}(T)$ for a given fissioning system.

TABLE III. Temperature-corrected and normalized values of the single-particle correction energies.

Energy	^{232}Th(n,f) (MeV)	^{238}U(n,f) (MeV)
Temperature-corrected values		
$\Delta E_{SP1}(T)$	0.64	1.04
$\Delta E_{SP2}(T)$	-4.79	-6.06
$\Delta E_{SP1}(T)-\Delta E_{SP2}(T)$ (calculated)	5.43	7.10
$\Delta E_{SP1}(T)-\Delta E_{SP2}(T)$ (experimental)	5.81	6.25
Values normalized to the experimentally derived value of $\Delta E_{SP1}(T)-\Delta E_{SP2}(T)$		
$\Delta E_{SP1}(T)$	0.68	0.92
$\Delta E_{SP2}(T)$	-5.13	-5.33

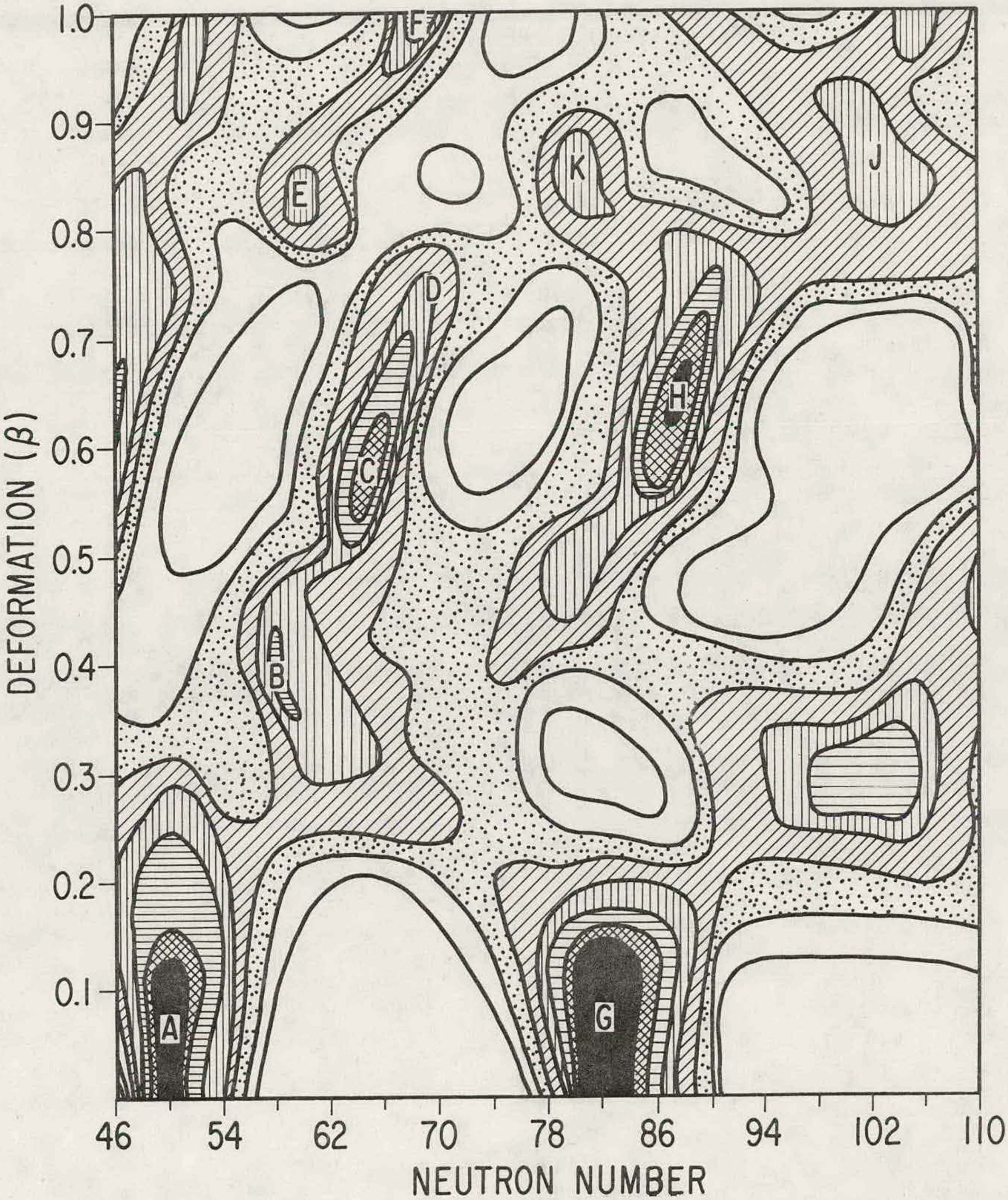
DEFORMATION (β)
1.0
0.9
0.8
0.7
0.6
0.5
0.4
0.3
0.2
0.1
A
B
C
D
E
F
G
H
J
K
46
54
62
70
78
86
94
102
110
NEUTRON NUMBER

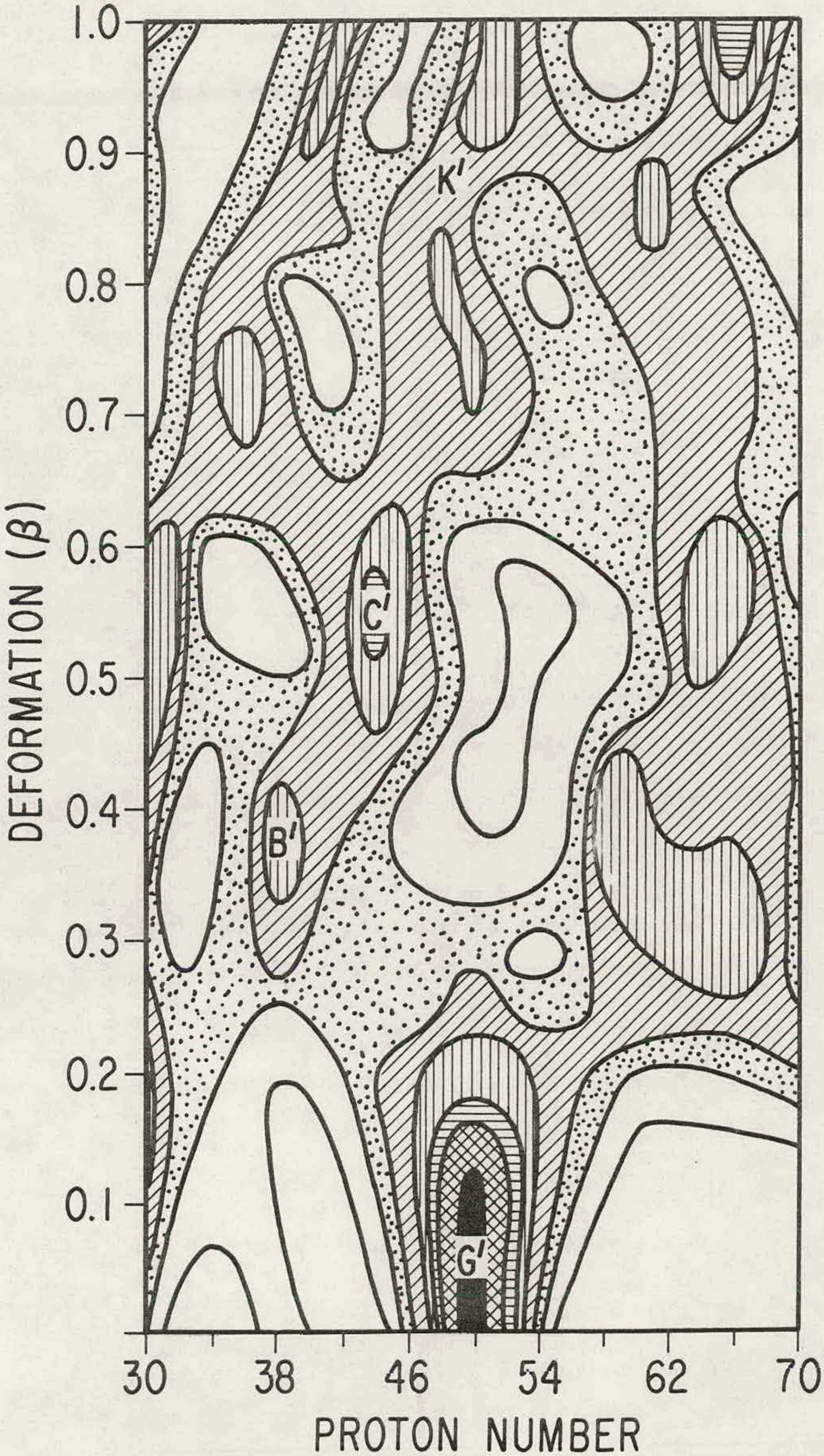
1.0
0.9
0.8
0.7
0.6
0.5
0.4
0.3
0.2
0.1
DEFORMATION (β)
30
38
46
54
62
70
PROTON NUMBER
K'
C'
B'
G'

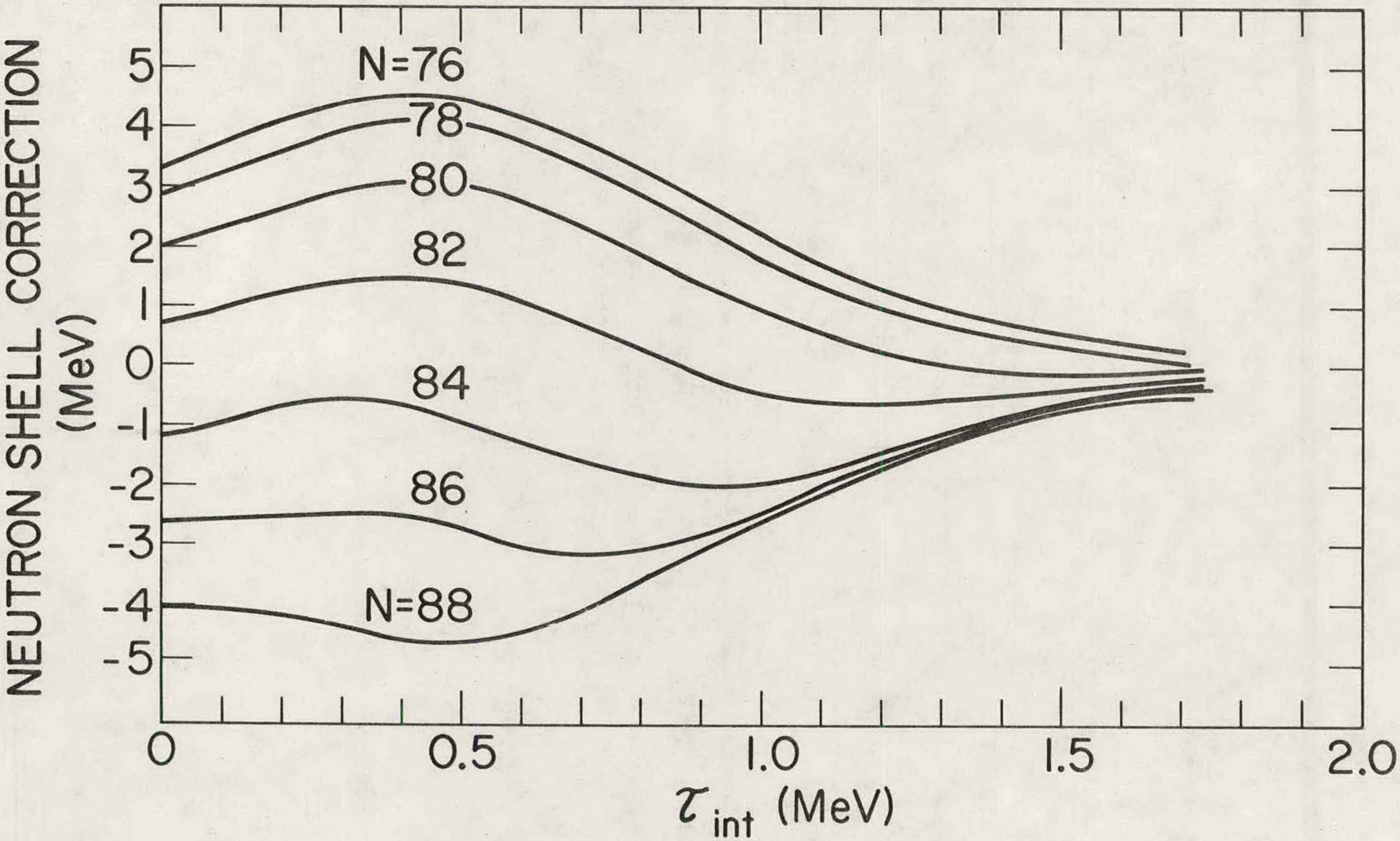
NEUTRON SHELL CORRECTION (MeV)
5
4
3
2
1
0
-1
-2
-3
-4
-5
N=76
78
80
82
84
86
N=88
0
0.5
1.0
1.5
2.0
τ_{int} (MeV)

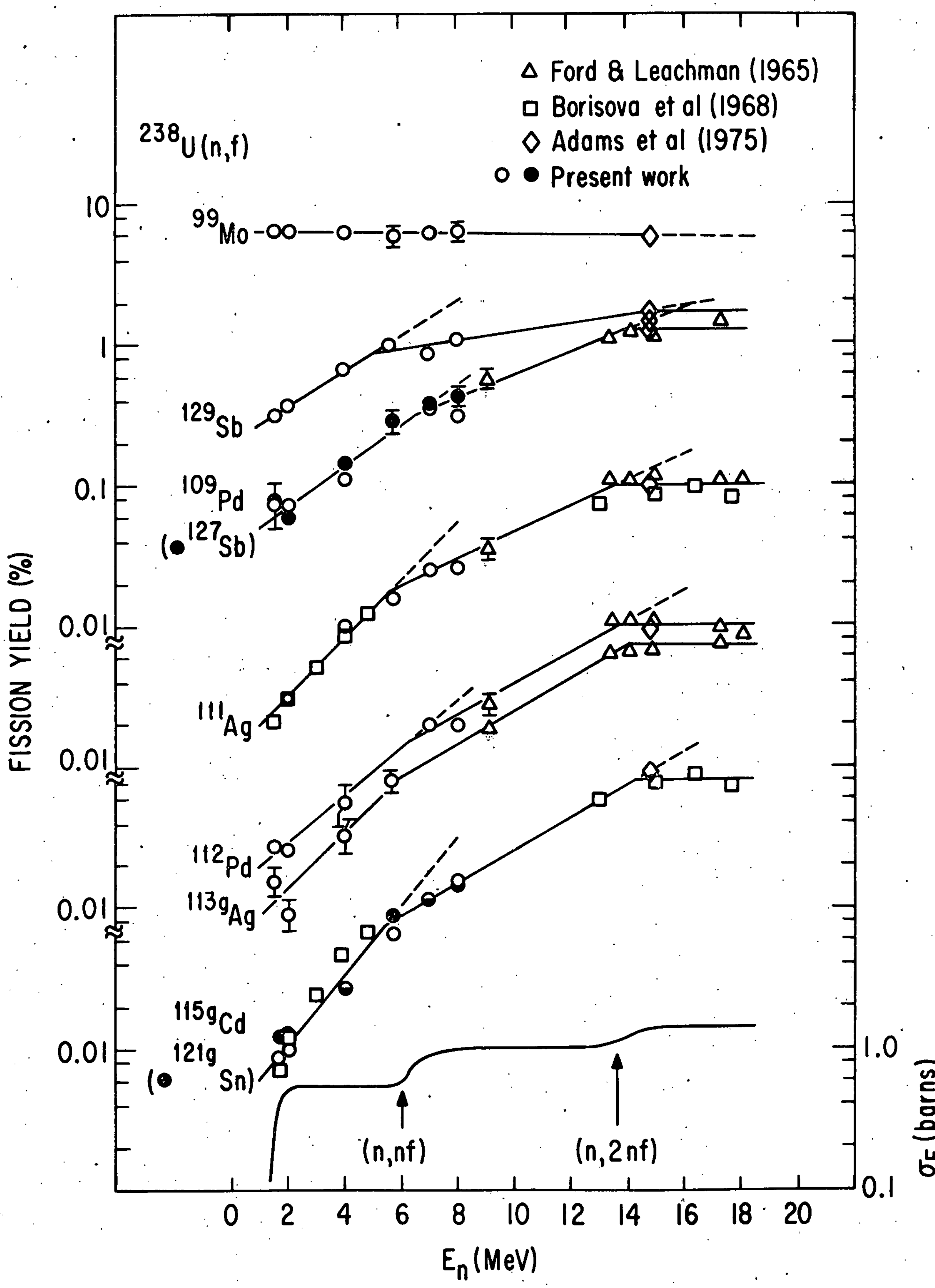
Ford & Leachman (1965)
Borisova et al (1968)
Adams et al (1975)
Present work
^{238}U(n,f)
10
1
0.1
0.01
0.01
0.01
0.01
^{99}Mo
^{129}Sb
^{109}Pd
(^{127}Sb)
^{111}Ag
^{112}Pd
^{113g}Ag
^{115g}Cd
(^{121g}Sn)
FISSION YIELD (%)
(n,nf)
(n,2nf)
1.0
0.1
σ_F (barns)
0
2
4
6
8
10
12
14
16
18
20
E_n (MeV)

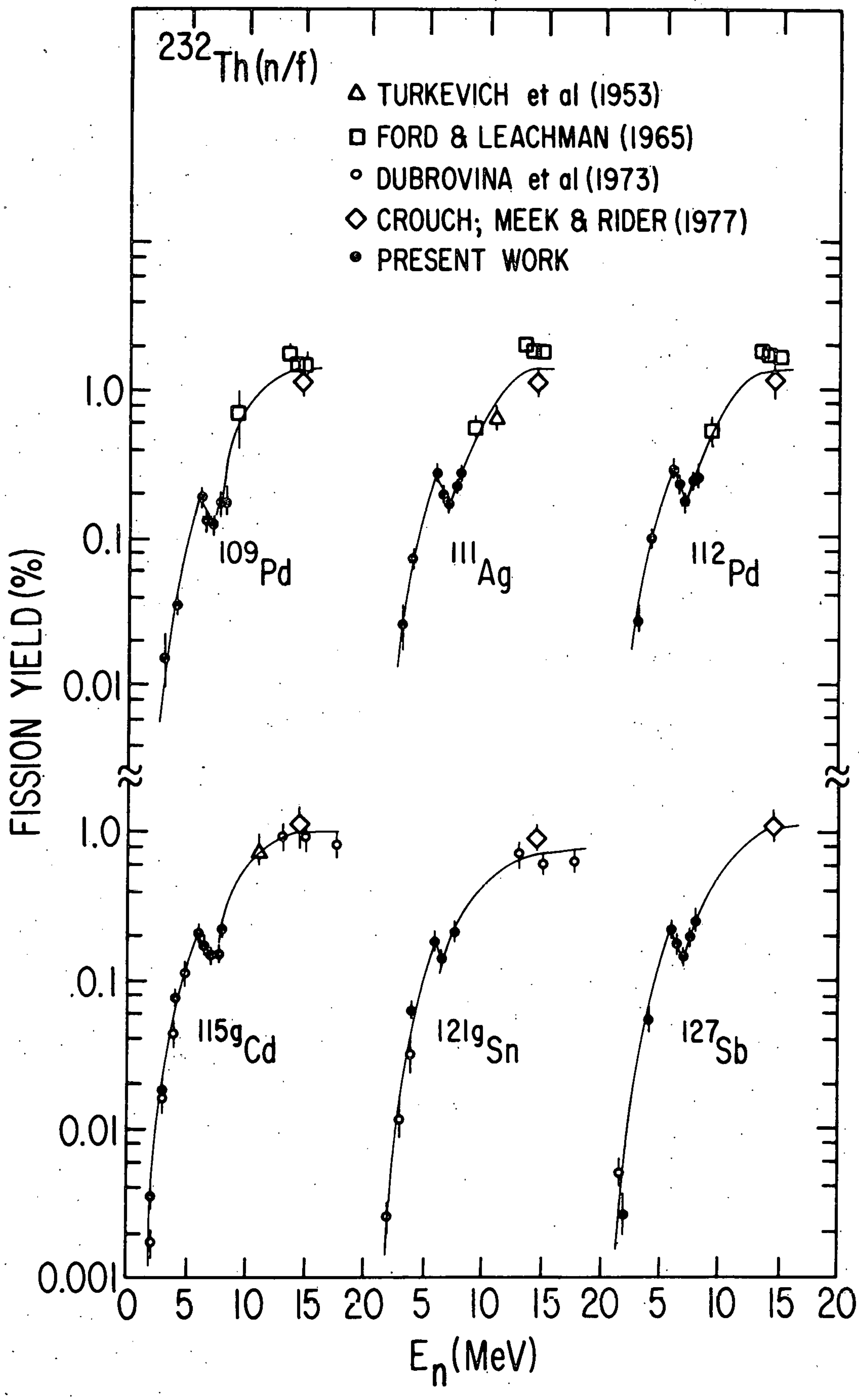

^{232}Th(n/f)
△ TURKEVICH et al (1953)
□ FORD & LEACHMAN (1965)
○ DUBROVINA et al (1973)
◇ CROUCH; MEEK & RIDER (1977)
● PRESENT WORK
^{109}Pd
^{111}Ag
^{112}Pd
^{115g}Cd
^{121g}Sn
^{127}Sb
FISSION YIELD (%)
E_n (MeV)

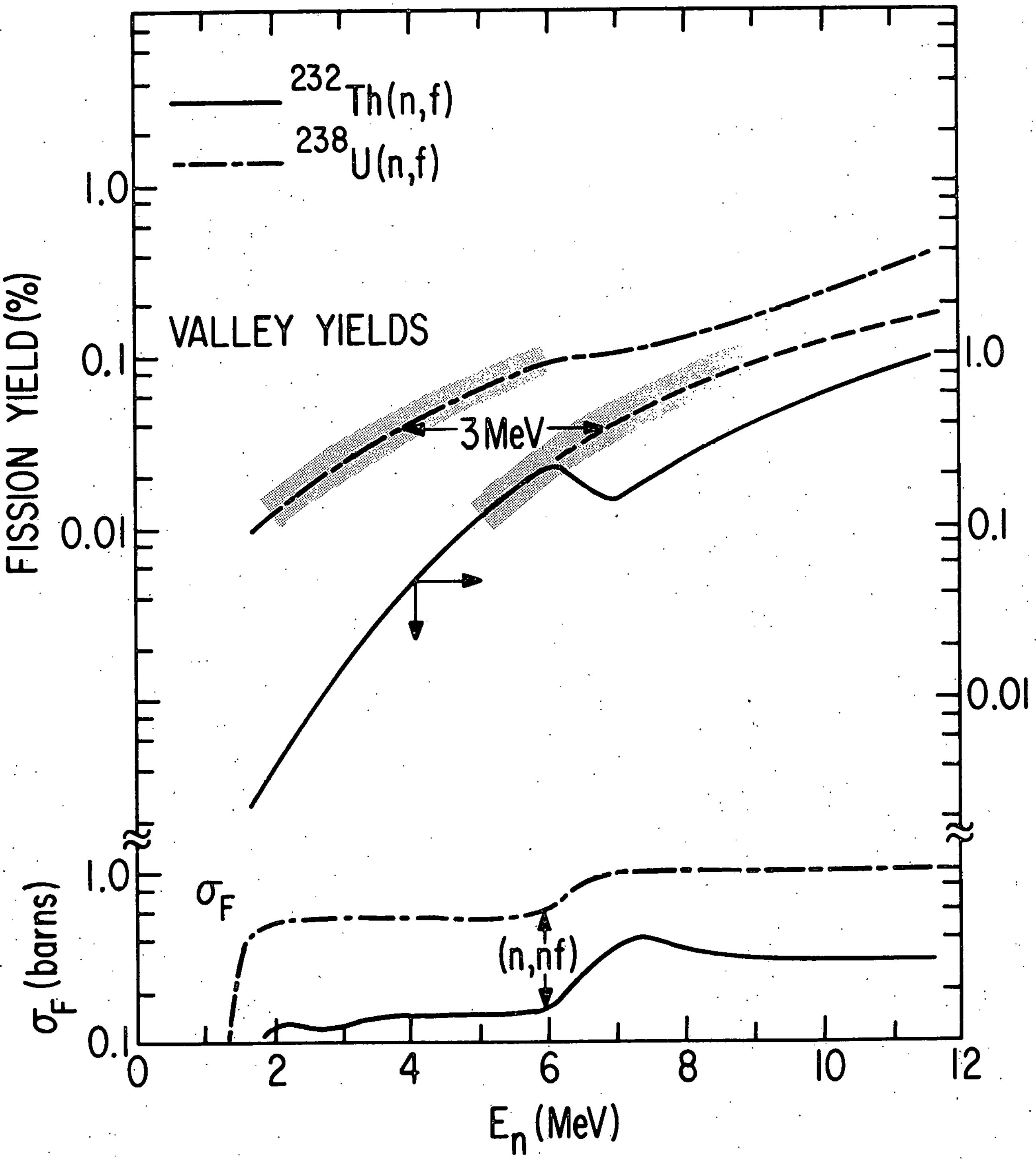

232Th(n,f)
238U(n,f)
1.0
0.1
0.01
FISSION YIELD (%)
VALLEY YIELDS
3 MeV
1.0
0.1
0.01
1.0
0.1
σF
σF (barns)
(n,nf)
0
2
4
6
8
10
12
En (MeV)

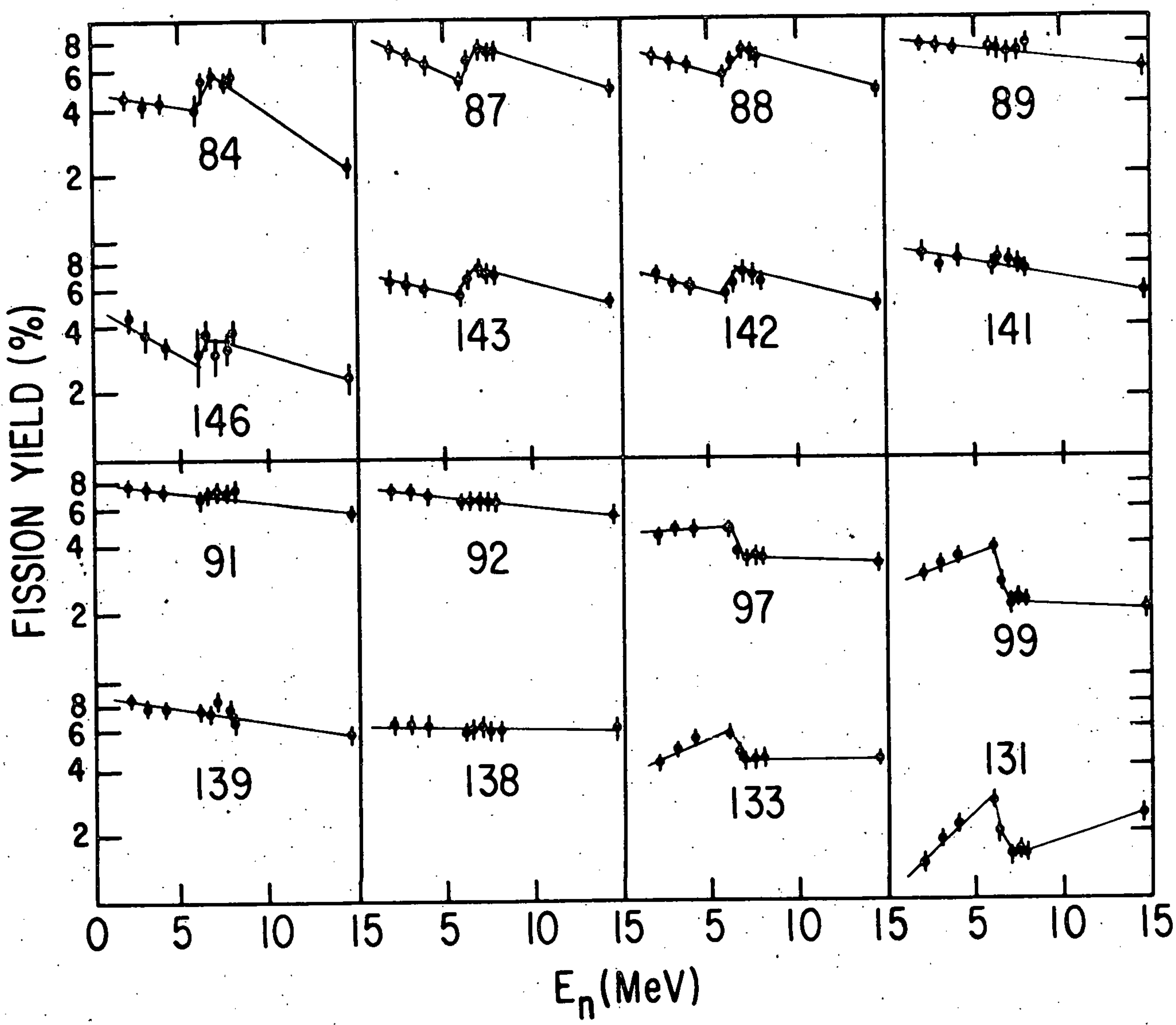

FISSION YIELD (%)
84
87
88
89
146
143
142
141
91
92
97
99
139
138
133
131
E_n (MeV)
0 5 10 15 5 10 15 5 10 15 5 10 15
8 6 4 2

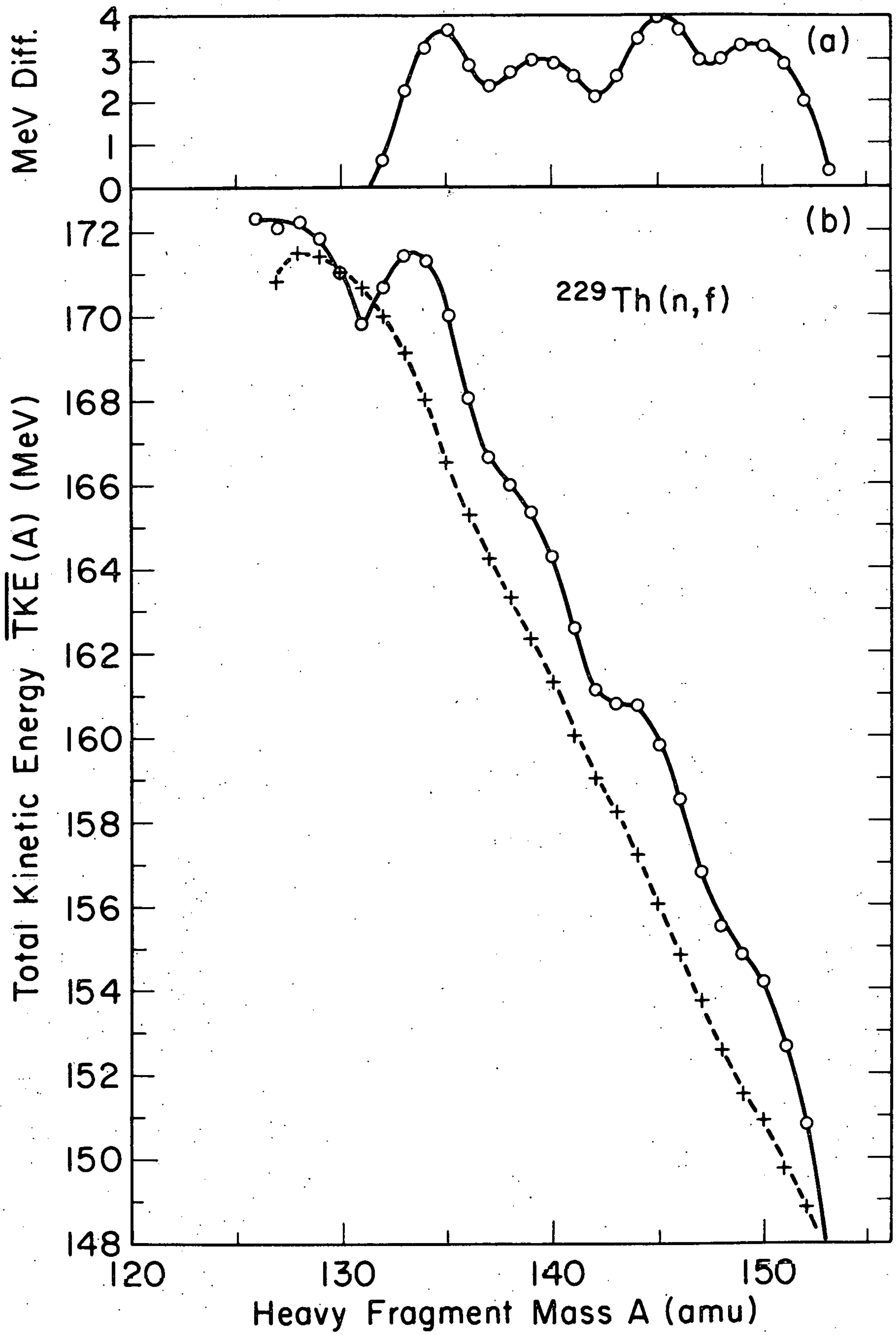

(a)
MeV Diff.
0
1
2
3
4
(b)
^{229}Th(n,f)
Total Kinetic Energy $\overline{TKE}$(A) (MeV)
148
150
152
154
156
158
160
162
164
166
168
170
172
120
130
140
150
Heavy Fragment Mass A (amu)

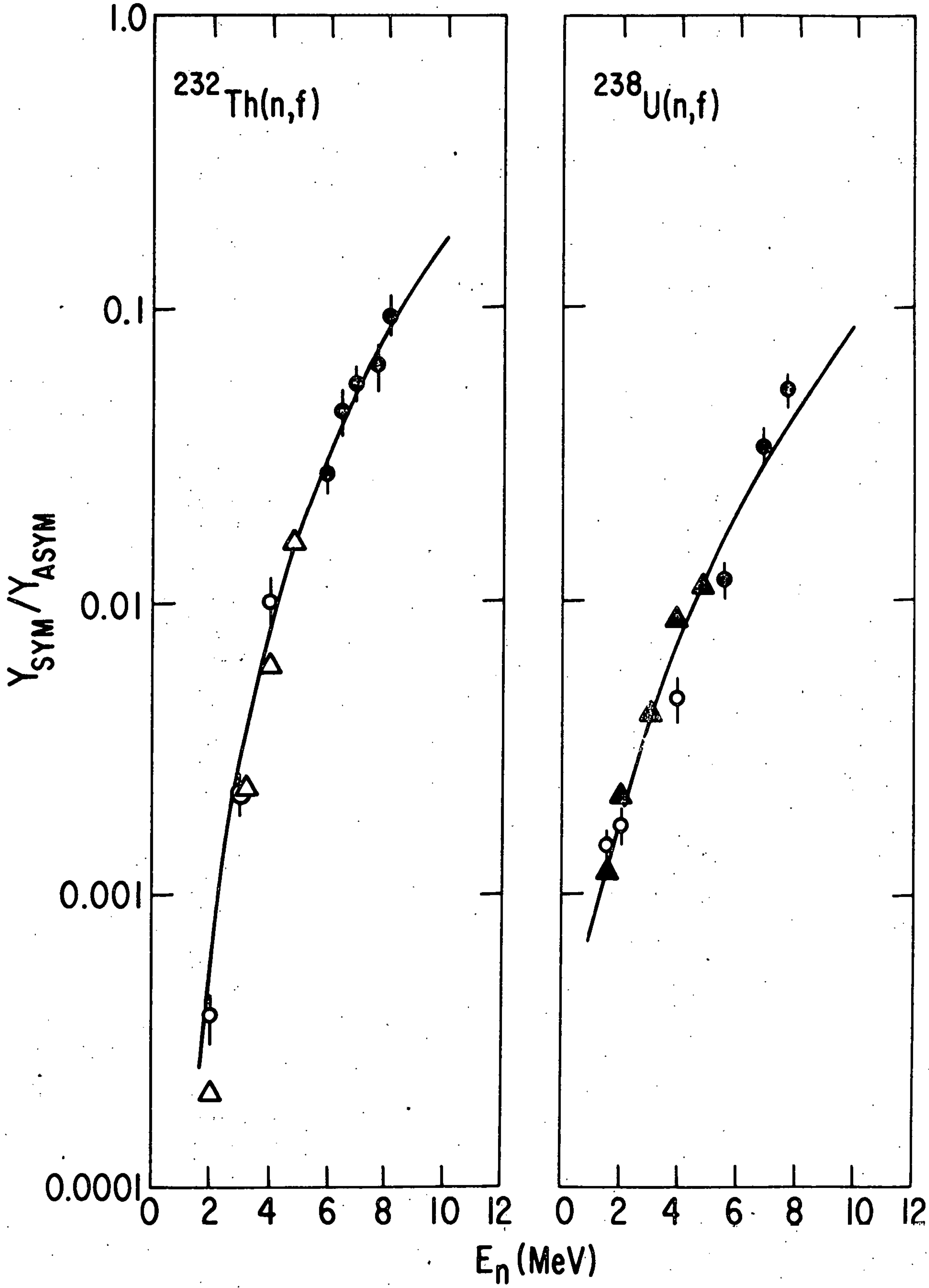

1.0
0.1
0.01
0.001
0.0001
^{232}Th(n,f)
^{238}U(n,f)
Y_{SYM}/Y_{ASYM}
0 2 4 6 8 10 12
0 2 4 6 8 10 12
E_n (MeV)

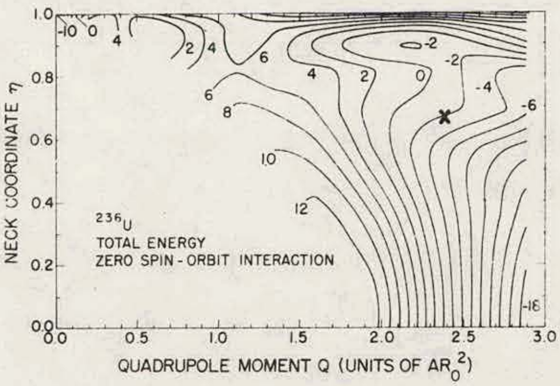
236U
TOTAL ENERGY
ZERO SPIN-ORBIT INTERACTION
NECK COORDINATE η
QUADRUPOLE MOMENT Q (UNITS OF AR0^2)